

Investigation of the LTC fuel performance index for oxygenated reference fuel blends

The Faculty of Oregon State University has made this article openly available.
Please share how this access benefits you. Your story matters.

Citation	Niemeyer, K. E., Daly, S. R., Cannella, W. J., & Hagen, C. L. (2015). Investigation of the LTC fuel performance index for oxygenated reference fuel blends. <i>Fuel</i> , 155, 14-24. doi:10.1016/j.fuel.2015.04.010
DOI	10.1016/j.fuel.2015.04.010
Publisher	Elsevier
Version	Accepted Manuscript
Terms of Use	http://cdss.library.oregonstate.edu/sa-termsfuse

Investigation of the LTC fuel performance index for oxygenated reference fuel blends

Kyle E. Niemeyer^{a,*}, Shane R. Daly^a, William J. Cannella^b, Christopher L. Hagen^c

^a*School of Mechanical, Industrial, and Manufacturing Engineering
Oregon State University, Corvallis, OR 97331, USA*

^b*Chevron Energy Technology Company
Richmond, CA, 94802, USA*

^c*School of Mechanical, Industrial, and Manufacturing Engineering
Oregon State University–Cascades, Bend, OR 97701, USA*

Abstract

A new metric for ranking the suitability of fuels in LTC engines was recently introduced, based on the fraction of potential fuel savings achieved in the FTP-75 light-duty vehicle driving cycle. In the current study, this LTC fuel performance index was calculated computationally and analyzed for a number of fuel blends comprised of *n*-heptane, isooctane, toluene, and ethanol in various combinations and ratios corresponding to octane numbers from 0 to 100. In order to calculate the LTC index for each fuel, computational driving cycle simulations were first performed using a typical light-duty passenger vehicle, providing pairs of engine speed and load points. Separately, for each fuel blend considered, single-zone naturally aspirated HCCI engine simulations with a compression ratio of 9.5 were performed in order to determine the operating envelopes. These results were combined to determine the varying improvement in fuel economy offered by fuels, forming the basis for the LTC fuel index. The resulting fuel performance indices ranged from 36.4 for neat *n*-heptane (PRF0) to 9.20 for a three-component blend of *n*-heptane, isooctane, and ethanol (ERF1). For the chosen engine and chosen conditions, in general lower-octane fuels performed better, resulting in higher LTC fuel index values; however, the fuel performance index correlated poorly with octane rating for less-reactive, higher-octane fuels.

Keywords: Low-temperature combustion, HCCI engines, Gasoline, Octane number

1. Introduction

Low-temperature combustion (LTC) strategies offer the potential of improved fuel economy and reduced pollutant emissions, both necessary to meet the increasing demands of federal regulations. Although LTC concepts such as homogeneous charge compression ignition (HCCI) engines have received significant research attention since first introduced [1, 2]—and continue to receive attention, albeit alongside related concepts such as reactivity controlled compression ignition (RCCI) [3–6] that varies fuel reactivity by stratifying a lower reactivity fuel like gasoline with a highly reactive fuel like diesel—a number of research challenges remain. In particular, unlike spark-ignition (SI) and compression-ignition (CI) engines where the spark and fuel injection initiate combustion, respectively, in HCCI and related engine concepts complex autoignition chemistry controls combustion timing. As a result, since the fuel chemistry plays a stronger role, varying fuel composition can result in a significantly different and potentially smaller range of operation in HCCI engines. In addition, while the lower combustion temperatures of HCCI combustion offers reduced nitrogen oxide (NO_x) emissions, it also results in high levels of carbon monoxide and unburned hydrocarbons [7]. Yao et al. [7] reviewed these and additional challenges in HCCI engine research, and the various strategies under investigation to solve them.

Early studies on HCCI strategies with gasoline [1, 2, 8] found that successful HCCI combustion could only be achieved in limited operating ranges. With a typical SI compression ratio, at low loads and while

*Corresponding author

Email address: Kyle.Niemeyer@oregonstate.edu (Kyle E. Niemeyer)

idling the knock resistance of typical high-octane gasoline prevents the initiation of autoignition; on the other hand, knocking can occur at higher loads. Diesel fuel, on the other hand, is much more reactive than gasoline and ignites too early when used in a premixed charge at the high compression ratios typical of CI engines [9]. While strategies to use typical gasoline and diesel fuels in HCCI engines have been investigated [7, 9], another option is to find new fuels or fuel blends that may offer more attractive performance. Various groups studied the operating ranges of different fuels in HCCI engines with the goal of identifying attractive species or mixtures [10–23]. The fuels studied include—but are not limited to—real fuels such as gasoline [10, 11, 17, 20–22], diesel [10, 18, 20], and Jet B [18]. In addition, numerous studies focused on neat fuels and mixtures of such, including *n*-butane [11], neat and blends of the primary reference fuels (PRFs) *n*-heptane and isooctane [10–13, 16, 17, 19, 22, 23], and mixtures of the PRFs with toluene [22, 23] and ethanol [17, 22, 23] both individually and together [23]. Other groups investigated the behavior of alcohols in HCCI engines, including neat butanol [20] and ethanol [20, 24–26]; wet ethanol also received significant attention as a neat fuel due to the potential for increased overall energy efficiency by avoiding or reducing distillation and dehydration [27–29]. The low reactivity of alcohols such as ethanol and methanol motivated additional research into operating HCCI engines using blends with more reactive fuels/additives such as *n*-heptane [30], diethyl ether [31, 32], dimethyl ether [33–36], and di-tertiary butyl peroxide [37]. In the opposite direction, other efforts studied injecting water into the engine cylinder to temper the reactivity of highly reactive fuels [33, 38–41]. However, nearly all of these efforts focused on a small subset of fuels and a narrow range of operating conditions; furthermore, a robust method to rank—and potentially predict—fuel performance in HCCI and other LTC-strategy engines has not yet emerged.

The octane rating, typically given by the research octane number (RON) and/or motor octane number (MON), is used to rank the resistance to knock of a gasoline-like fuel in SI engines, where a higher number indicates greater knock resistance. These values are determined by comparing the knocking characteristics under standardized conditions to those of a binary mixture of the PRFs *n*-heptane and 2,2,4-trimethylpentane (isooctane), where 0 and 100 correspond to the volume percentage of *n*-heptane and isooctane, respectively. However, various studies showed that octane rating does not adequately predict autoignition in HCCI engines [14, 15, 22, 23], due to the fact that real fuels consist of more complex mixtures of fuel components compared to the PRFs.

A number of new metrics have been proposed to better quantify fuel performance in HCCI engines. Kalghatgi [14] first introduced the octane index, which combines the RON and MON values for a fuel with an empirical parameter related to engine-specific operating conditions. Later, Shibata and Urushihara [15] developed three HCCI fuel indices, including the relative HCCI index that combines MON with information about the fuel composition. However, as Rapp et al. [22] recently showed in a study of the performance of various fuels in a Cooperative Fuel Research (CFR) engine operating in HCCI mode, neither of the octane or relative HCCI indices can predict the autoignition behavior for a wide range of fuels. In particular, the correlations for both indices poorly predict the behavior of gasoline blends with naphthenes, aromatics, and ethanol. Truedsson et al. [23] recently presented another number for specifying fuel performance in HCCI engines: the Lund–Chevron HCCI Number, based on the required compression ratio for autoignition at a particular combustion phasing.

However, while the various existing indices partially succeed in describing the combustion behavior of gasoline-like fuels in HCCI engines, none relate the fuel performance to fuel savings in realistic engine conditions. This motivates the development of a new metric for measuring the performance of fuels in LTC engines in order to both rank fuels and predict future performance. Such a metric could also be used to identify attractive fuels for HCCI engine operation or assist in the development of new fuels. Niemeyer et al. [42] recently introduced a novel LTC fuel index that combines information about the fuel operating envelope—the feasible engine speeds and loads for a fuel in HCCI mode—with the operating conditions needed under realistic engine operation. As such, this LTC index ranks poorly fuels with wide operating ranges that are outside the conditions needed for typical vehicles in typical driving conditions, because using such a fuel in an HCCI engine would have a minimal impact on overall fuel consumption.

By gauging the impact of various fuels on real-world fuel economy via transient driving cycles, the current approach is distinct from the (significant) prior efforts focused on advanced internal combustion engine development. However, certain studies summarized here used transient driving cycles to predict fuel economy and emissions improvements using advanced engine modes such as HCCI and related concepts. Zhao et al. [43] simulated a hybrid SI/HCCI gasoline engine through the European New Emission Drive

Cycle, although they reported achieving only moderate improvements in fuel economy and emissions due to the limited range of operating conditions in HCCI mode. Curran et al. [44] used five steady-state modal points [45, 46] to approximate the EPA Federal Test Procedure (FTP-75) driving cycle, then compared fuel economy and emissions of RCCI, diesel HCCI, and conventional diesel combustion by performing engine experiments over the set of conditions. Similarly, Ortiz-Soto et al. [47] developed an engine and vehicle modeling framework that they used to simulate a hybrid SI/HCCI engine-powered vehicle over the EPA UDDS, Highway Fuel Economy Test, and US06 driving cycles. Using similar methodologies to the above efforts, Gao et al. [48] and Ahn et al. [49] modeled hybrid-electric vehicles capable of conventional/HCCI operation. Both studies found that while conventional vehicles benefit from HCCI operation in terms of fuel consumption and emissions, HCCI offered little improvement to hybrid-electric vehicles due to its limited operation range in the higher loads where the electric motor was not needed. Unlike the current work, the studies cited here studied the performance of typical gasoline fuels over the driving cycles, rather than exploring the performance of various fuels or seeking to find new fuels that might offer wider HCCI operating envelopes.

The current study builds on an earlier effort [42] that introduced a new LTC fuel performance index by determining the indices for a number of fuel blends comprised of *n*-heptane, isooctane, toluene, and ethanol in various combinations and ratios. The range of fuels investigated here is similar to that studied by Truedsson et al. [23, 50–52] in their experiments on the compression ratio required for autoignition; however, unlike the current computational approach those experiments held equivalence ratio and engine speed constant. Following the general procedure first introduced by Niemeyer et al. [42], we performed driving cycle simulations for a typical light-duty passenger vehicle to generate steady-state operating points in terms of engine speed and torque, and also obtained the corresponding baseline SI engine fuel consumption for these operating points. Next, HCCI engine simulations were performed for a variety of fuel blends in order to determine their operating ranges. The resulting operating envelopes were combined with the necessary operating points for the driving cycle, and we then calculated the LTC fuel index for each blend studied by considering the potential fuel savings achieved by switching to HCCI combustion for the feasible operating points.

In the following sections, we first describe in detail the methodology for calculating our fuel performance index, including vehicle driving cycle simulations, fuel HCCI operating envelope simulations, and the index calculation. Next, we present and discuss results of operating envelope and index calculations for oxygenated reference fuel mixtures. Finally, we summarize our study and describe future directions for this work.

2. Methodology

The overall process for calculating the proposed LTC fuel performance index consists of three steps: (1) driving cycle simulations for a model vehicle to obtain engine operating information, (2) HCCI engine simulations for various fuels to obtain operating envelopes, and (3) the combination of the data from the previous two steps to calculate the LTC fuel index. This process is depicted visually in Fig. 1, and described in detail in the following sections.

2.1. Driving cycle simulation

In order to determine necessary fuel operating ranges for HCCI combustion, we performed simulations of a light-duty passenger vehicle in the US EPA FTP-75 driving cycle [53]. The FTP-75 driving cycle attempts to emulate typical urban driving conditions with a short cold start phase, a transient phase, and a hot start phase; it is used to measure the fuel economy and emissions of passenger cars in the United States. It covers a total distance of 17.8 km in 1874 s (not including a 10 min break beginning at 1367 s), with an average vehicle speed of 34.1 km/h.

We chose the Toyota Camry—the best-selling passenger car in North America in recent years—for the modeled vehicle as a representative of typical light-duty vehicles in North America. In order to simulate the performance—and the fuel consumption in particular—of this vehicle over the driving cycle, we used the ADvanced VehIcle SimulatOR (ADVISOR) [54, 55] package. ADVISOR is a hybrid backward/forward-facing vehicle simulator, meaning that it combines elements of backward-facing models, which start from the tractive force needed to move the vehicle at the directed speed, and forward-facing models, which start from a driver directing the engine to meet the necessary speed, to calculate fuel economy and emissions of

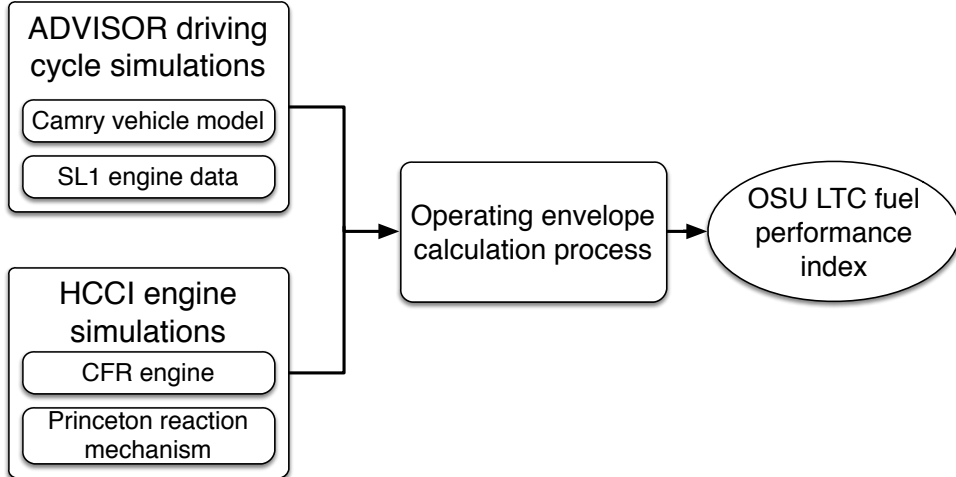


Figure 1: Flowchart describing the LTC fuel performance index calculation process.

various vehicles over specified driving cycles. See Wipke et al. [54] or Gao et al. [56] for more details on such models. ADVISOR interpolates data from experimental engine maps of steady-state fuel consumption rates and emissions, based on engine speed and torque, to model performance in the transient driving cycle.

We simulated the vehicle by modifying ADVISOR’s default model for a small passenger car, VEH_SMCAR, which is based roughly on a 1994 Saturn SL1. The altered model, VEH_SMCAR_CAMRY, includes reference and estimated parameters for a 2012 Toyota Camry: coefficient of drag of 0.28, frontal area of 2.28 m², fraction of vehicle weight on front axle of 0.54, vehicle center-of-gravity height of 0.53 m, vehicle wheelbase of 2.775 m, and vehicle curb weight of 1447 kg. Coupled with this vehicle model, we used the FC_SI95 engine model, which is based on the Saturn 1.9 L dual overhead cam SI engine with a compression ratio of 9.5. This model includes maps of fuel use and emissions based on the experimental data of Reilly et al. [57]. We scaled the model engine from the default maximum power of 95 kW to 133 kW, to more closely match the Camry’s engine for which data was not readily available.

Driving cycle calculations performed by ADVISOR return pairs of engine speed and torque in one second intervals. In order to compare these load requirements to the fuel operating envelopes described in the next section, the following basic relation for four-stroke engines estimated the corresponding brake mean effective pressure (bmep):

$$\text{bmep} = \frac{4\pi T}{V_d}, \quad (1)$$

where T indicates the torque and V_d the volume displaced per cycle [58].

Next, in order to fairly compare engines of different sizes, we obtained the indicated mean effective pressure (imep) by accounting for the total friction work dissipated in the engine, including pumping, rubbing friction, and accessory work, using

$$\text{imep} = \text{bmep} + \text{tfmep}, \quad (2)$$

where tfmep is the total friction mean effective pressure. This can be obtained using the empirical relationship for four-stroke four-cylinder SI engines given by Heywood [58, 59]:

$$\text{tfmep} = 0.97 + 0.15 \left(\frac{N}{1000} \right) + 0.05 \left(\frac{N}{1000} \right)^2, \quad (3)$$

where tfmep is measured in bar and N is the engine speed measured in revolutions per minute. While updated friction correlations are available that reflect decreased friction losses in modern engines and incorporate more factors [60–63], we used the correlation of Eq. (3) to match the age of the SI engine used for the driving cycle simulations [57]. In addition, no detailed in-cylinder information was available from the ADVISOR-based driving cycle simulations, preventing the use of more sophisticated correlations.

2.2. Fuel operating envelope

Next, in order to determine the fuel operating envelopes we modeled an HCCI engine using the single-zone internal combustion engine model of CHEMKIN version 10131 [64]. Rather than matching the engine of the Toyota Camry, we simulated the well-studied CFR engine, avoiding dependence of results on engine size by using imep instead of torque to compare engine performance between the driving cycle simulations and work output from the HCCI engine simulations (as will be described shortly). We emulated the CFR engine using the following geometry taken from Rapp et al. [22]: a cylinder displacement volume of 0.616 L, connecting rod to crank radius ratio of 4.44, and cylinder bore diameter of 82.8 mm. Simulations were performed from intake valve close to exhaust valve open, corresponding to 146° BTDC and 140° after top dead center (ATDC) [11]. For the current study, we selected a compression ratio of 9.5 to match that of the SI engine used for the experimental data. All simulations were performed with naturally aspirated intake conditions and with standard valve timing (i.e., no negative valve overlap [65, 66]). In addition, to partially address the differences between the engine used for experimental data and the modeled CFR engine, we quantified load using imep as described previously.

In order to model heat loss through the cylinder walls, we used the typical Woschni heat transfer correlation [58]:

$$Q_{\text{wall}} = hA(T - T_{\text{wall}}) \quad (4)$$

$$\text{Nu} = \frac{hB}{\lambda} = 0.035\text{Re} \quad (5)$$

$$\text{Re} = \frac{Bw\rho}{\mu} \quad (6)$$

where $w = 2.28\bar{S}_p$ is the average cylinder gas velocity from Yelvington et al. [12], $\bar{S}_p = 2LN$ is the mean piston speed, N is the engine speed, ρ is the density, and L and B are the cylinder stroke and bore as given above. CHEMKIN approximates the gas conductivity λ and viscosity μ using an empirical power-law relationship [64]. For all cases, we used a wall temperature of 430 K as given for a CFR engine by Flowers et al. [67].

As in the previous section for torque, we converted the indicated work reported by CHEMKIN to imep, in order to readily compare the calculated fuel operating envelopes to the engine operating points given for the driving cycle by ADVISOR:

$$\text{imep} = \frac{W_{c,i}}{V_d}, \quad (7)$$

where $W_{c,i}$ represents the indicated work per cycle.

Using the results from simulations that varied engine speed and fuel-air equivalence ratio, we next determined which cases corresponded to satisfactory HCCI combustion using operating limits criteria. Operational limits for HCCI engines are typically based on knock/ringing at the high-load limit and misfire/incomplete combustion at the low-load limit [68, 69]. Here, the upper limit for HCCI operation is defined as a maximum pressure rise rate ($dP/d\theta$) of 20 bar/(° CA) [11, 70]. However, Eng [71] first showed that this quantity may not be appropriate due to its dependence on operating parameters (e.g., engine speed, intake pressure), and suggested a limit based on ringing intensity [25, 71, 72]; future work will explore using such a criteria.

Experimentally, the low-load misfire limit is typically determined using a threshold on the coefficient of variation in imep; however, in idealized simulations such instabilities do not occur and a limit based on, e.g., the combustion efficiency must be used [68]. We defined the lower (misfire) limit as 90% molar conversion of C from fuel to CO₂, corresponding to incomplete combustion [73, 74]. Figure 2 shows sample pressure traces for HCCI simulations of PRF0 (*n*-heptane) at a compression ratio of 9.5, initial temperature of 330 K, initial pressure of 1 atm, and an engine speed of 1400 rpm, with representative examples of knock, normal combustion, and misfire using the described limits.

In addition to these combustion limits, rather than select particular initial conditions, a restriction on the combustion timing through a constant CA50 value—the crank angle degree at which 50% of the total heat release has occurred—ensured acceptable combustion phasing. For all fuels, we varied the initial temperature with the compression ratio and initial pressure held constant to keep CA50 at $3 \pm 2^\circ$ ATDC [23, 50–52, 75, 76]. Note that combustion timing control was not considered in the examples of Fig. 2.

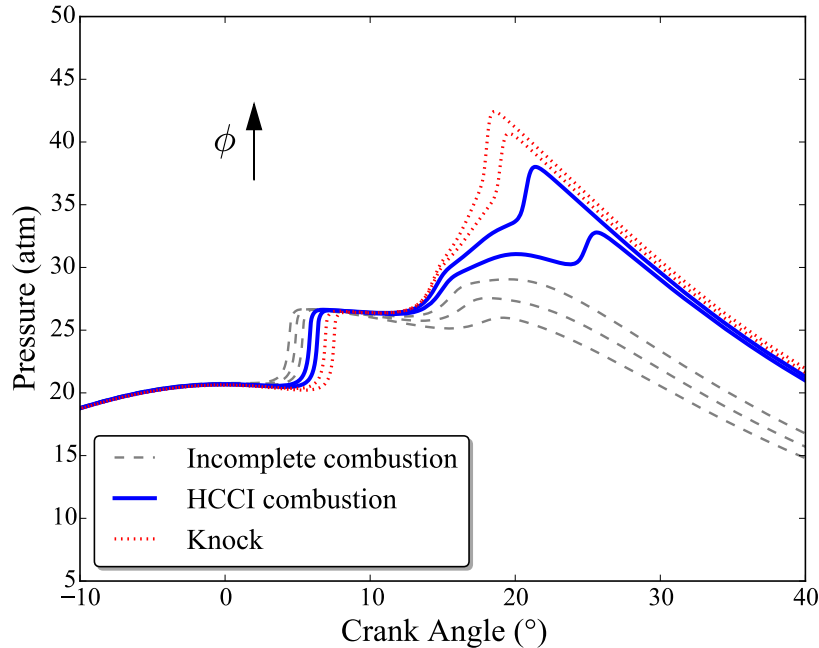


Figure 2: Representative pressure traces for PRF0 (*n*-heptane) HCCI combustion at CR = 9.5, initial temperature of 330 K, initial pressure of 1 atm, 1400 rpm, and varying equivalence ratios, demonstrating knocking combustion, normal combustion, and misfire.

Practically, the value of CA50 was determined in this work by cumulatively integrating the net heat release rate per degree—given by CHEMKIN—using the composite trapezoidal rule to obtain the heat released as a function of crank angle. This result is then interpolated to find the crank angle associated with 50% of the total heat release, using third-, second-, and first-order spline interpolations in order (if the initial higher-order fit resulted in an interpolation error); a linear interpolation was used if all attempted spline interpolations failed. These calculations were implemented in Python using the SciPy functions `scipy.integrate.cumtrapz` and `scipy.interpolate.interp1d`, respectively [77].

2.3. LTC fuel performance index

By combining the results from the driving cycle simulations with the HCCI operating envelopes obtained for various fuels, we constructed a novel fuel performance index based on the potential fuel economy improvement offered by a fuel; it contains information about both the size and location of operating envelopes. Fuels with wide operating limits that also match ranges of operation important to real-world driving conditions will offer a greater real-world reduction in fuel consumption and therefore should be highly ranked. Due to a varying HCCI operation range, where SI operation would be required outside of the viable operating envelope, different fuels offer varying levels of fuel economy improvement.

The LTC fuel index is defined as the percentage of fuel savings achieved through HCCI operation; in other words, the fuel savings “actually” achieved normalized by the potential fuel savings. First, we can calculate the potential fuel savings for full HCCI operation, $m_{f,s,HCCI}$, based on the baseline SI fuel consumption over the entire driving cycle, $m_{f,SI}$:

$$m_{f,HCCI} = (1 - \alpha)m_{f,SI} , \quad (8)$$

$$m_{f,s,HCCI} = m_{f,SI} - (1 - \alpha)m_{f,SI} , \quad (9)$$

$$= \alpha m_{f,SI} , \quad (10)$$

where α represents the potential improvement in fuel economy offered by HCCI combustion over SI combustion (e.g., 0.15–0.2 [9], 0.3 [43]) and $m_{f,HCCI}$ is the fuel consumption for full HCCI operation. The SI

fuel consumption $m_{f,SI}$ is obtained from the ADVISOR driving cycle simulation, which reports the fuel consumption rate $\dot{m}_{f,SI}$ in one second intervals. Recognizing the limited operating range offered by HCCI, the fuel saved during hybrid SI/HCCI operation, $m_{f,s,SI+HCCI}$, is given by

$$m_{f,s,SI+HCCI} = m_{f,SI} - m_{f,SI+HCCI} , \quad (11)$$

$$= \alpha m_{f,SI \in \{HCCI\}} , \quad (12)$$

where $m_{f,SI+HCCI}$ is the fuel consumed over the hybrid SI/HCCI operation and $m_{f,SI \in \{HCCI\}}$ is the fuel consumed during the baseline SI operation over the possible HCCI operating range. In other words, the fuel saved during the hybrid SI/HCCI operation is determined only by the fuel consumed during SI operation at the HCCI-viable operating points—the rest of the driving cycle is unaffected.

In order to obtain the mass of fuel consumed during SI operation for a particular fuel’s HCCI operating envelope, we form a convex hull of the fuel HCCI operating points using a Delaunay triangulation [77, 78]. Then, each of the driving cycle engine operating points is tested for being within the bounds of the hull. Finally, the corresponding fuel mass consumption data for points within the operating envelope are summed to give $m_{f,SI \in \{HCCI\}}$.

The fuel index is then defined as the percentage of fuel savings achieved:

$$I_{LTC} = \frac{m_{f,s,SI+HCCI}}{m_{f,s,HCCI}} \cdot 100\% , \quad (13)$$

$$= \frac{\alpha m_{f,SI \in \{HCCI\}}}{\alpha m_{f,SI}} \cdot 100\% , \quad (14)$$

$$= \frac{m_{f,SI \in \{HCCI\}}}{m_{f,SI}} \cdot 100\% . \quad (15)$$

Note the cancellation of the fuel savings factor α in Eq. (14). The index I_{LTC} can also be interpreted as the mass-weighted percentage of discrete operating points for viable HCCI combustion. Therefore, the fuel index can be calculated independent of a specific HCCI fuel consumption improvement factor, although a constant improvement factor across the range of operating conditions is implicitly assumed.

2.4. Limitations to approach

Note that since engine simulations covered the compression and expansion strokes of the cycle, the gross indicated work per cycle was used. The approach presented here is also unable to predict transient phenomena in the engine between the operating points, or switching from SI to HCCI operation. Gao et al. [79] developed a methodology to estimate transient effects from steady-state engine data, and used this to improve predictions of fuel consumption and emissions in vehicle driving cycle simulations. Nüesch et al. [80] also developed a model to predict transient effects from switching between the SI and HCCI combustion modes, finding that fuel consumption increased during transitions enough to nearly cancel out the HCCI improvements, and determined optimal timing delays to reduce these negative effects.

Finally, the single-zone HCCI simulations used here assume spatial homogeneity, with no ability to capture spatial variations. In order to deal with this limitation, a number of engine modeling approaches have been developed that—while avoiding the cost of a spatially resolved, multidimensional computational fluid dynamics simulation—consider multiple zones to represent different regions within an engine (e.g., core, piston crevice, boundary layer) [74, 81–84]. While these multi-zone models can more closely match experimental results, particularly for heat release rate, peak pressure, and unburned hydrocarbon emissions, the single-zone model adequately predicts the point of ignition as a function of inlet properties [83]. Furthermore, Yelvington et al. [12] showed that single-zone calculations could be used to accurately predict knock limits for HCCI combustion.

Noting these limitations, the current work is focused on demonstrating the methodology of constructing the fuel index and showing calculations for various fuel blends. Therefore, the computational results are not quantitatively compared with experiments, but rather only to each other in order to study trends and the relative performance of various fuels.

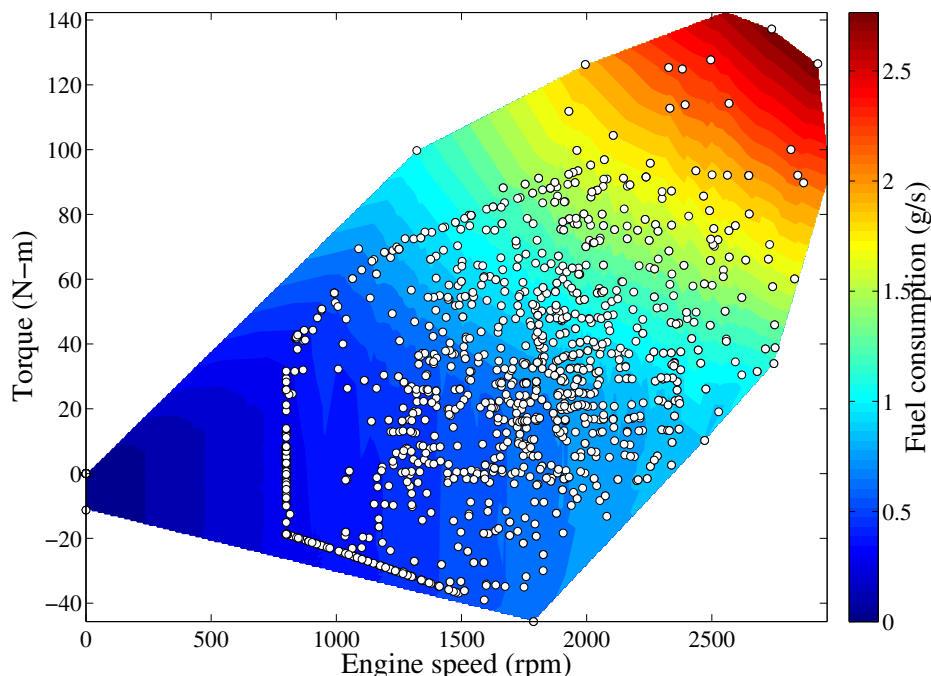


Figure 3: Engine speed and torque operating points with fuel consumption rate overlaid for simulated driving cycle.

3. Results and discussion

First, ADVISOR was used to simulate the performance of the model Camry vehicle over the FTP-75 driving cycle. Figure 3 shows the resulting engine speed and torque operating points for the driving cycle. In addition, the fuel consumption rate in g/s is overlaid on the points. As expected, Fig. 3 demonstrates higher fuel consumption rates at higher loads and engine speeds. Note that negative torque values occurred for this vehicle and driving cycle combination, corresponding to vehicle deceleration. While these points contributed to fuel economy due to nonzero fuel consumption rates—365 out of 2478 total operating points, or 12.4% of the total fuel consumption—our current HCCI engine model is not able to produce negative torque/imep values. Therefore, at best a fuel can currently achieve $I_{LTC} = 87.6$.

Next, we used engine simulations to determine the HCCI operating ranges for a variety of multicomponent fuels consisting of *n*-heptane, isooctane, toluene, and ethanol, including binary, ternary, and quaternary mixtures. In order to search for operating points that corresponded to viable HCCI combustion over the specified driving cycle, these simulations were performed by varying equivalence ratio from 0.18–0.45 for all the fuels. We used the Princeton detailed reaction mechanism for TERF mixtures [85–88] for all the HCCI engine simulations.

3.1. Operating envelopes and fuel indices

Table 1 lists information about the fuels considered in the study, including their RON/MON values and molar composition in terms of the four neat components, as well as their calculated LTC fuel indices (I_{LTC}). In addition, the table reports percent coverage of driving cycle operating points. Where necessary, mole fractions were obtained from given volume fractions using the `vol-to-mole` utility [89].

Figures 4, 5, 6, and 7 show the operating envelopes of the various PRFs, binary blends of *n*-heptane with toluene and ethanol, three-component toluene reference fuels (TRFs) and ethanol reference fuel (ERF), and four-component toluene ethanol reference fuels (TERFs), respectively, converted to imep and compared to the engine operating points for the driving cycle. Clearly, PRF0 (*n*-heptane) offers the largest operating envelope, although it does not cover numerous driving cycle operating points at the very low and high loads. Interestingly, the operating envelopes of PRF55–PRF100 seem to converge on a similar location, which is

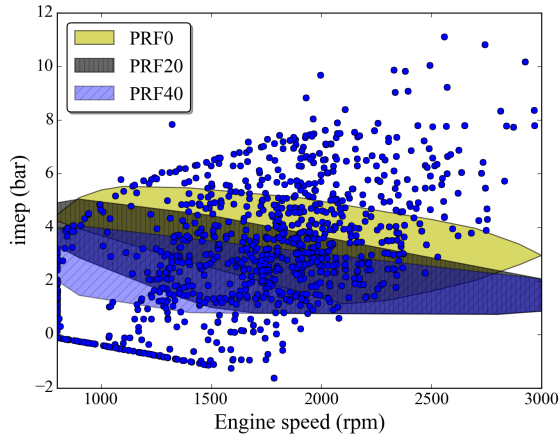
Fuel	RON/MON	X_H	X_I	X_T	X_E	% pts.	I_{LTC}
PRF0	0/0	1.0	–	–	–	25.3	36.4
PRF20	20/20	0.816	0.184	–	–	23.5	29.0
PRF40	40/40	0.625	0.375	–	–	19.0	22.0
PRF55	55/55	0.476	0.524	–	–	26.6	21.2
PRF70	70/70	0.322	0.678	–	–	23.0	17.4
PRF85	85/85	0.164	0.836	–	–	22.9	17.4
PRF100	100/100	–	1.0	–	–	8.60	9.39
H90T10	14.1/12.6	0.867	–	0.133	–	24.1	31.4
H80T20	27.7/24.8	0.744	–	0.256	–	22.2	26.6
H60E40 [52, 75]	71.4/65.0	0.374	–	–	0.626	28.3	22.5
TRF1 [93]	39.0/37.0	0.6379	0.1418	0.2203	–	16.0	18.1
TRF2 [94]	88.8/84.8	0.17	0.56	0.28	–	9.93	10.6
TRF3 [93]	76.2/70.9	0.3061	0.2727	0.4222	–	22.5	17.4
TRF4 [51, 75]	82.8/80.7	0.2085	0.6477	0.1438	–	8.92	10.0
ERF1 [52, 75]	78.7/76.7	0.2769	0.4915	–	0.2317	8.15	9.20
TERF1 [51, 75]	67.1/63.7	0.3764	0.3758	0.1298	0.1181	24.3	18.5
TERF8 [51, 75]	71.8/65.8	0.3445	0.1911	0.3564	0.1081	24.3	18.5
TERF14 [51, 75]	74.8/68.9	0.3242	0.1978	0.2236	0.2543	24.8	18.8

Table 1: List of fuels considered in the study and their performance, with octane numbers, molar compositions (X_H , X_I , X_T , and X_E refer to isooctane, *n*-heptane, toluene, and ethanol, respectively), percentage of operating point coverage, and HCCI index calculations. RON/MON values for the H90T10, H80T20, and TRF2 blends were calculated using the correlation given by Morgan et al. [93]. References indicate the source of the mixture, where applicable.

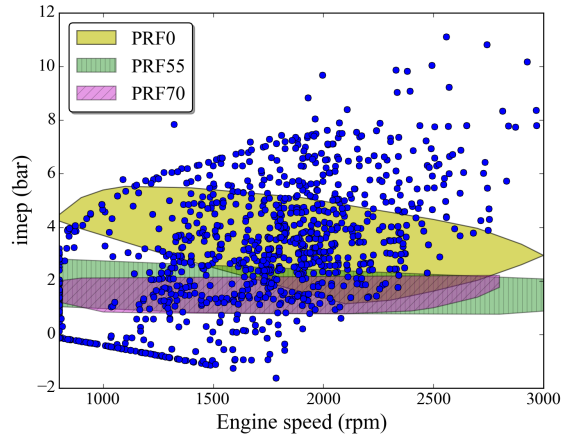
also mostly shared by TRF2–TRF4, ERF1, and all three TERFs. Therefore, for the current compression ratio and CA50 target, fuels with octane ratings above 55 appear limited to HCCI operation for imep loads of 0–3 bar.

While it is somewhat difficult to compare these results for the fuel HCCI operating envelopes with experimental results from the literature due to the difference in techniques, multiple experimental studies observed some of the same trends found here. For example, Atkins and Koch [13] found experimentally that increasing octane number corresponded to reduced operating envelope size for PRF20, PRF40, and PRF60, operating with a compression ratio of 12, engine speed of 700 rpm, and varying equivalence ratios. Aroonsrisopon et al. [11] demonstrated similar trends experimentally for PRF70 and PRF91.8. On the other hand, these and other studies showed that higher-octane PRFs had narrower but higher-load operating ranges [11, 13, 70]; in our study, while increasing octane rating did result in narrower operating ranges for fuels—both PRFs and more complex blends—it also led to operating at lower loads. We attribute these opposing trends to the difference in approaches: whereas our approach focused on holding combustion timing (i.e., CA50) constant by varying initial temperature, those experimental efforts held temperature constant [42] demonstrated the same trends as the experimental studies. Rapp et al. [22] studied the ranges of HCCI operation for various fuels, but varied compression ratio and reported the ranges in terms of CA50 while holding engine speed constant at 600 rpm. Truedsson et al. [23] performed a similar study holding engine speed constant and reporting the operating range in terms of compression ratio required for autoignition, with a target CA50 of $3 \pm 1^\circ$.

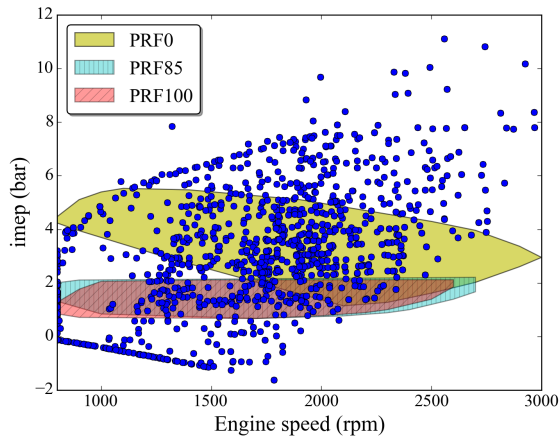
Finally, based on the results shown in Figs. 4–7, the LTC fuel performance indices for all the fuels were calculated using Eq. (15) and are shown in Table 1. As expected based on the wide operating range shown in Fig. 4, PRF0 (*n*-heptane) showed the highest index at 36.4 while ERF1 gave the lowest performance at 9.20. Figure 8 shows the LTC fuel indices tabulated in Table 1 plotted against the fuels’ RON and MON. Clearly, neither RON nor MON can completely explain the variation in index for all the fuels studied here. For higher reactivity fuels (RON/MON < 40), the fuel index starts at the highest observed value for RON/MON = 0 and decreases linearly with RON/MON. However, for RON/MON \geq 40 the calculated fuel indices



(a) PRF0, PRF20, PRF40



(b) PRF0, PRF55, PRF70



(c) PRF0, PRF85, PRF100

Figure 4: Operating envelopes for PRF mixtures at $CR = 9.5$ and naturally aspirated inlet conditions over FTP-75 driving cycle. PRF0 (*n*-heptane) is repeated in each figure for perspective.

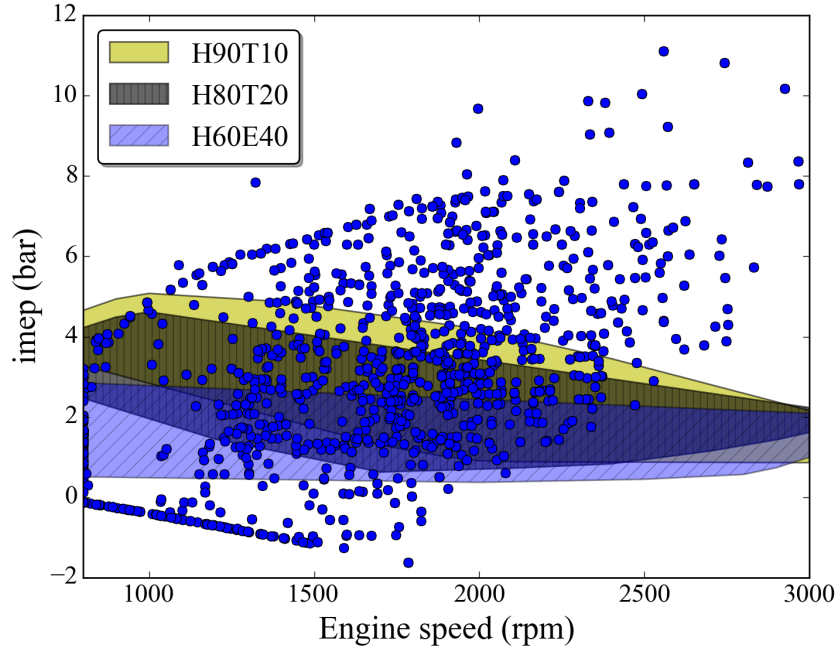


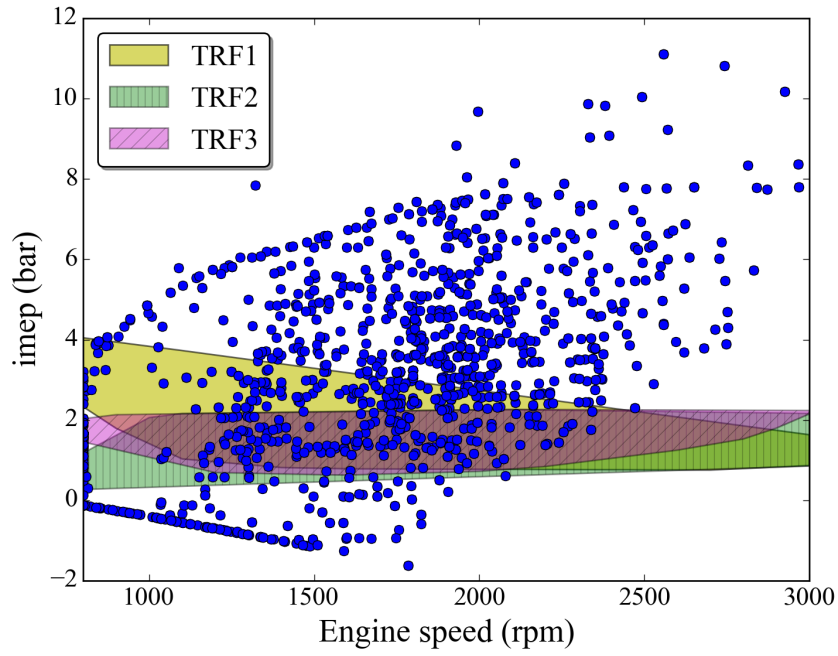
Figure 5: Operating envelopes for binary mixtures of *n*-heptane with toluene (H80T20 and H90T10) and ethanol (H60E40) at CR = 9.5 and naturally aspirated inlet conditions over FTP-75 driving cycle.

do not correlate well with octane number—fuels with similar RON or MON, but different composition, demonstrate different fuel indices. For example, fuels with RON/MON of approximately 70–80 demonstrate indices ranging from 9 to nearly 23. These results further support the conclusion that octane number does not adequately predict fuel performance in HCCI engines, particularly for fuels with RON/MON of 40–90.

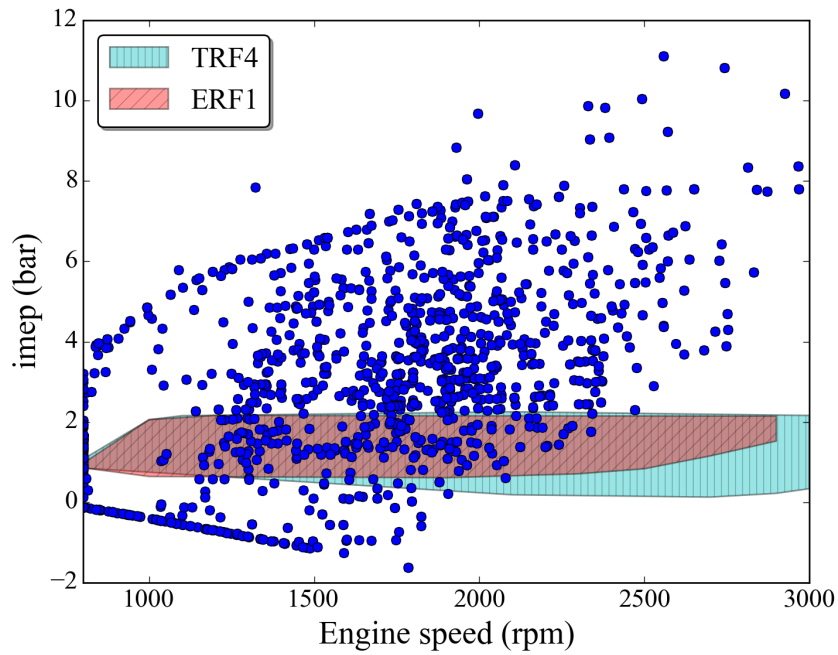
From the trends contained in Table 1 and shown in Fig. 8, a few observations can be made on the effects of different fuel components. For example, PRF70 and H60E40 contain similar amounts of *n*-heptane and have octane ratings near 70, but the fuel performance index of H60E40 is 29% higher. These results suggest that isooctane has a stronger negative affect on the fuel performance index than ethanol, when holding *n*-heptane composition constant. Similarly, PRF40 and TRF1 both have octane ratings of around 40 and approximately the same *n*-heptane content, but PRF40’s index is 22% higher. We attribute this result to the presence of toluene and reduced isooctane content of TRF1, suggesting that toluene more negatively affects the index than isooctane.

We did not attempt to compare our fuel index to those of Kalghatgi [14], Shibata and Urushihara [15], or Truedsson et al. [23]. All of these depend on specifying engine operating conditions such as a particular engine speed, intake temperature, or compression ratio in order to determine a fuel rating. As such, it would be difficult to compare these numbers with our fuel index due to the varying engine speeds and inlet temperatures used to emulate realistic engine operating conditions. We believe that basing a fuel performance rating on the wide range of engine speeds and loads experienced in practical conditions provides more useful information than attempting to emulate the traditional RON and MON tests with a single or limited test conditions as in the discussed prior efforts. However, we acknowledge the prior work done in this direction, and feel that our proposed approach represents the next step in terms of a fuel performance index, building on these prior efforts.

Finally, note that most fuels exhibited viable HCCI operation over the full range of engine speeds considered, with the exceptions of PRF70, PRF85, and PRF100. However, the location of these operating envelopes at higher engine speeds below the driving cycle operating points meant that no fuel savings were achieved for these locations, limiting the performance indices of these fuels. The ability of a fuel to support successful HCCI operation is necessary but not sufficient in order to improve fuel economy in realistic engine conditions—the operating envelope must cover practical engine speeds and loads.



(a) TRF1, TRF2, TRF3



(b) TRF4, ERF1

Figure 6: Operating envelopes for ternary TRF and ERF mixtures at $CR = 9.5$ and naturally aspirated inlet conditions over FTP-75 driving cycle.

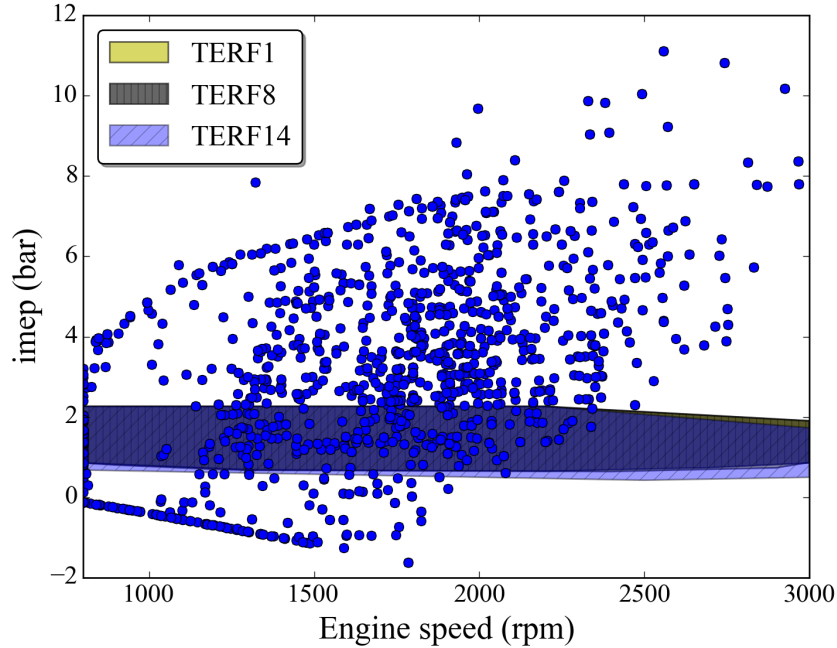


Figure 7: Operating envelopes for quaternary TERF mixtures at $CR = 9.5$ and naturally aspirated inlet conditions over FTP-75 driving cycle.

3.2. Validation of CA50 approach

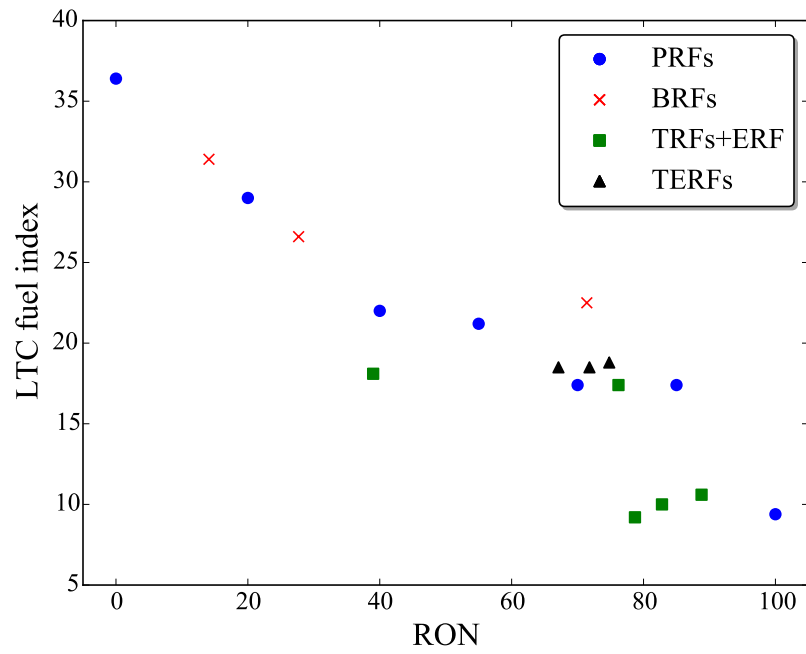
Next, we provide justification for the constant CA50 approach and the broad applicability of the current results by showing that, in general, the operating envelope for fuels in terms of imep is relatively consistent for a particular CA50 value regardless of the specific conditions (e.g., compression ratio, initial temperature) used to achieve that value. Figure 9 displays the range of viable HCCI operation for PRF70 using imep as a function of CA50, simultaneously varying compression ratio between 9.5 and 16 and initial temperature between 310–600 K over the range of engine speeds and equivalence ratios given previously. These results demonstrate that the operating envelope of a fuel in terms of imep (i.e., load) is mostly consistent for a given value of CA50—particularly for CA50 values in -5 – 10° ATDC—regardless of the combination of conditions used to achieve that timing. This observation starts to break down at the highest compression ratio of 16, which shows some higher-load operation than the other compression ratios.

These results also suggest the possibility of extending the HCCI operating ranges to higher or lower loads by either increasing or decreasing CA50, within the appropriate range for acceptable engine performance. Such a strategy for increasing the HCCI operating range—and therefore the LTC fuel index—will be the focus of future work.

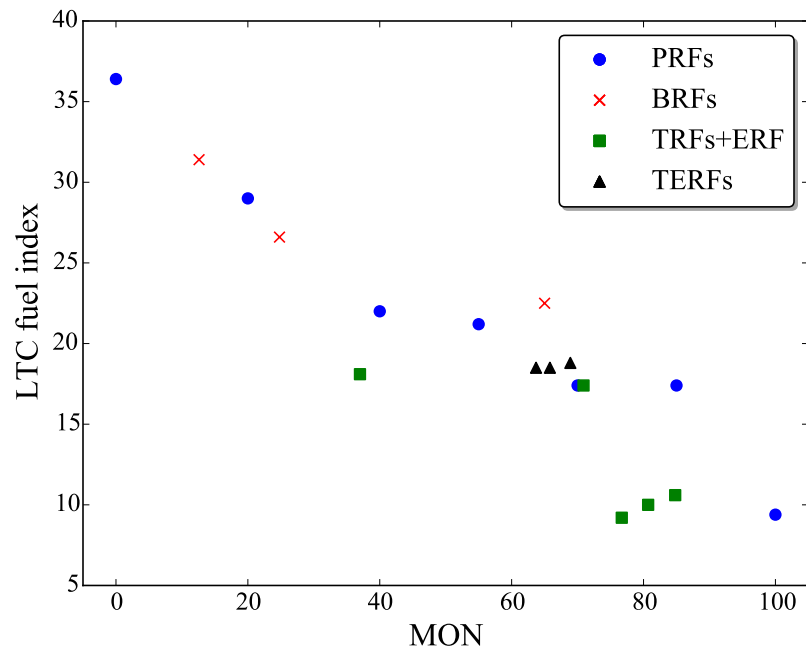
3.3. Sensitivity to CA50 value and tolerance

Previous efforts found the optimal CA50 within 2 – 10° ATDC for the best tradeoff between efficiency, emissions, and maximum brake torque [69, 90–92]. We selected $3 \pm 2^\circ$ ATDC based on similar values used in numerous recent studies [23, 50–52, 75, 76], which falls on the early side of the optimal timing range. However, as shown in Fig. 9 and discussed previously, higher CA50 values corresponding to later ignition timing may allow HCCI operation at higher loads. Since different engine loads correspond to varying fuel consumption, shifting CA50 up or down could impact the LTC fuel index.

Figure 10 shows the sensitivity of LTC fuel index (I_{LTC}) for PRF0 (*n*-heptane) and PRF70 to CA50 values over -7 – 15° ATDC. For PRF0, the data is shown as well as a quadratic fit, with the coefficient of determination $r^2 = 0.988$. The data indicate that the maximum fuel index occurs near 3° (3.34° as given by the maximum of the fit), coincidentally near our chosen CA50 value. The fuel index decreases as the ignition timing is shifted earlier or later; therefore, it is sensitive to the CA50 value. Figure 10 shows a similar CA50



(a) RON



(b) MON

Figure 8: Correlations between LTC fuel index and RON/MON, with symbols indicating the different fuel mixtures.

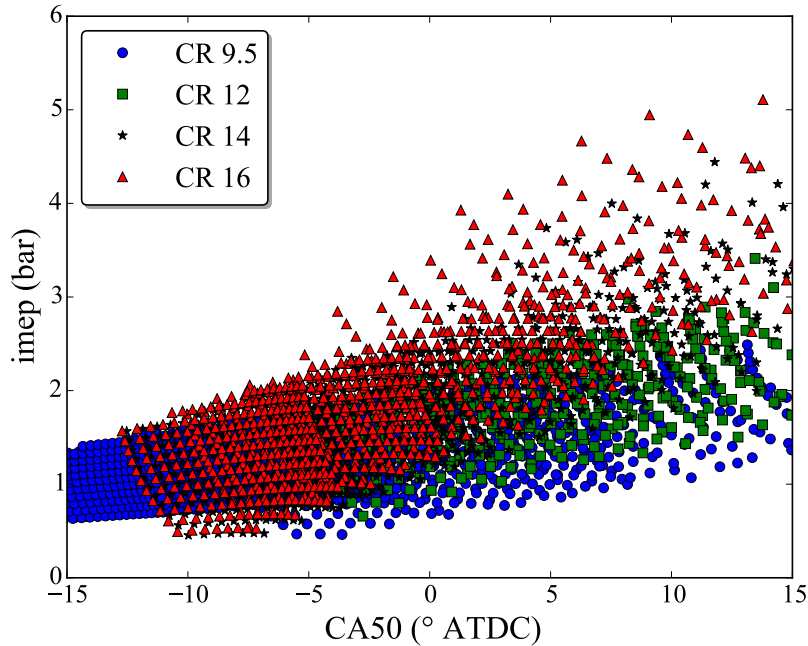


Figure 9: PRF70 operating range given in imep as a function of CA50 value, with varying compression ratios (as shown), engine speeds over 800–3000 rpm, equivalence ratios of 0.1–0.45, and initial temperatures over 310–600 K.

value sensitivity analysis for PRF70; although the variation is less well-behaved than PRF0, the LTC fuel index shows a similar dependence on CA50 value, with a maximum also occurring near 3° ATDC. In this case, the fuel index increases and decreases abruptly with shifting CA50 due to the particular location of the PRF70 operating envelope inside the driving cycle operating points.

The LTC fuel index could also be sensitive to the CA50 tolerance ($\pm 2^\circ$ here), in addition to the CA50 value itself. Figure 11 presents the sensitivity of LTC fuel index for PRF0 and PRF70 to CA50 tolerance, with the target value itself set to 3° ATDC. In both cases, the fuel performance index ranges from nearly zero at $\pm 0.01^\circ$ to around 50 and 20 for PRF0 and PRF70, respectively at $\pm 10^\circ$. Interestingly, the index values for both fuels respond similarly as the CA50 tolerance increases, although PRF70 exhibits a greater jump around $\pm 1^\circ$.

4. Conclusions

In this work, we developed a new metric to measure fuel performance in HCCI engines, based on the potential fuel economy improvement offered under realistic vehicle driving conditions. Different fuels offer varying ranges of HCCI operation, but a wide operating range alone does not guarantee real-world fuel savings—fuels with operating envelopes that cover practical engine speeds and loads should be favored. We obtained engine operating information by simulating the performance of a Toyota Camry, a popular passenger vehicle in North America, over the EPA FTP-75 (federal light-duty) transient driving cycle. Separately, we performed HCCI engine simulations for a variety of fuels in order to determine the variation in operating envelopes offered by each fuel. We then combined these data to create a fuel index measuring the percentage of fuel savings achieved, where 0 represents no fuel savings and 100 represents the full potential fuel savings achieved, corresponding to no viable HCCI operation and full HCCI combustion, respectively, over the driving cycle.

The HCCI operating envelopes for mixtures of *n*-heptane, isooctane, toluene, and ethanol were determined for a compression ratio of 9.5 and naturally aspirated intake conditions over a range of engine speeds and equivalence ratios, with combustion timing held constant at CA50 of $3 \pm 2^\circ$ by varying initial temperature to

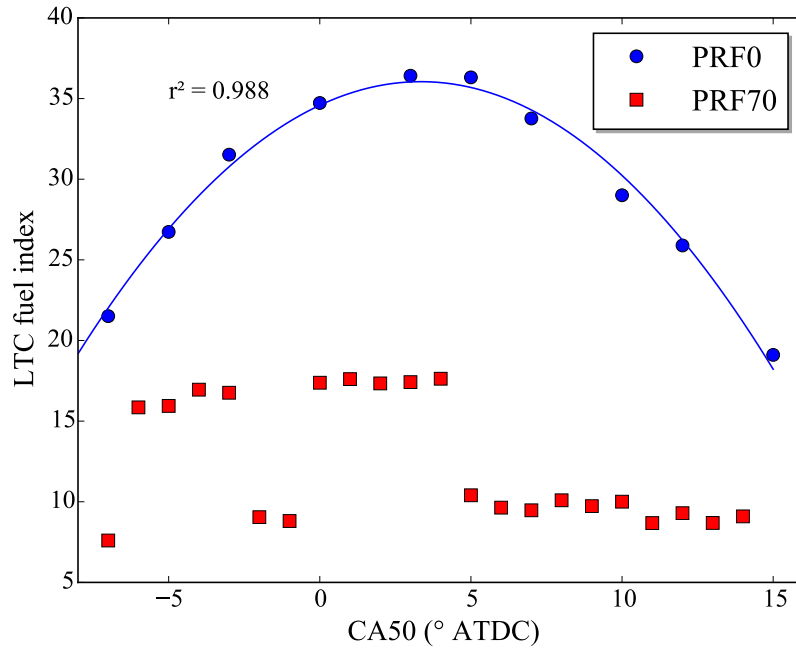


Figure 10: LTC fuel index for PRF0 and PRF70 with varying target CA50 value. Symbols indicate the actual points and the line is a quadratic fit with the coefficient of determination given as r^2 . PRF70 results have no obvious correlation.

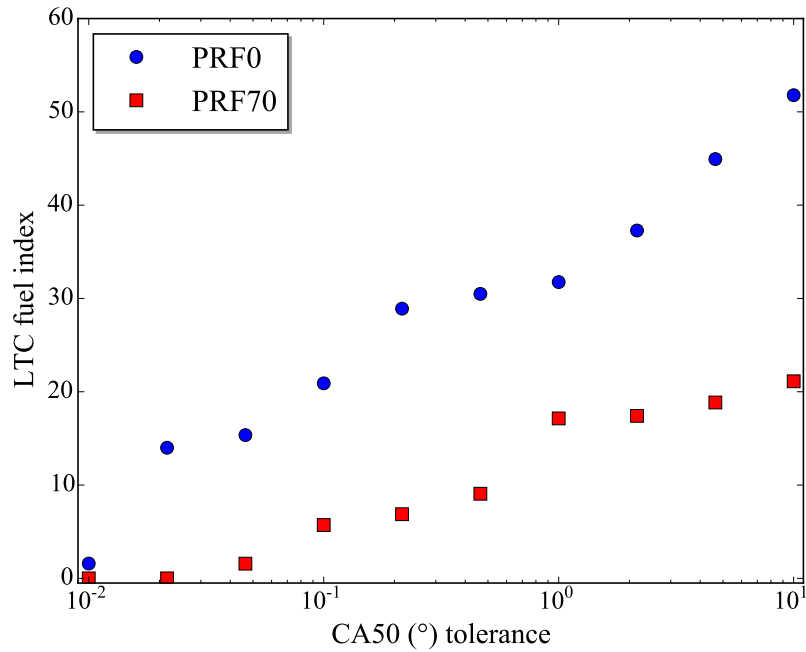


Figure 11: LTC fuel index for PRF0 and PRF70 with varying CA50 tolerance, centered around 3° ATDC. Note the logarithmic scale of the the horizontal axis.

emulate intake heating. In general, the results demonstrated that lower octane rating corresponded to wider operating ranges, and higher octane fuels converged on a similar low-load operating range for the chosen engine. By combining the necessary driving cycle engine speeds and with the PRF operating envelopes, the LTC fuel index I_{LTC} was calculated for each fuel. The lowest octane PRF considered (*n*-heptane) ranked highest using this metric, but the index value did not monotonically decrease with increasing octane number—consistent with literature results showing that octane number is not a sufficient metric for fuel performance in LTC engine modes. However, even the highest-performing fuel only demonstrated an index of around 36, indicating that it would only achieve 36% of the possible fuel savings in the driving cycle. Therefore, additional research needs to be performed into increasing the operating envelope of fuels for HCCI combustion.

The work presented here represents a stepping stone, and as such our future work involves investigating fuel operating envelopes at higher compression ratios and with pressure boosting, and considering additional fuel components necessary to emulate real gasoline. Furthermore, one possibility that merits further investigation for increasing the high-load limits of fuels in HCCI combustion is delaying the combustion timing. In addition, we will explore the dependence of the fuel index on the particular driving cycle selected by using, e.g., the New European Drive Cycle (NEDC) and Japanese JC08 tests.

Acknowledgments

The authors gratefully acknowledge the Chevron Energy Technology Company for supporting this research.

References

- [1] S. Onishi, S. Jo, K. Shoda, P. Jo, S. Kato, Active thermo-atmosphere combustion (ATAC) – a new combustion process for internal combustion engines, SAE Technical Paper 790501, 1979. doi:[10.4271/790501](https://doi.org/10.4271/790501).
- [2] P. M. Najt, D. E. Foster, Compression-ignited homogeneous charge combustion, SAE Technical Paper 830264, 1983. doi:[10.4271/830264](https://doi.org/10.4271/830264).
- [3] S. L. Kokjohn, R. M. Hanson, D. A. Splitter, R. D. Reitz, Experiments and modeling of dual-fuel HCCI and PCCI combustion using in-cylinder fuel blending, SAE Int. J. Engines 2 (2010) 24–39.
- [4] S. L. Kokjohn, R. M. Hanson, D. A. Splitter, R. D. Reitz, Fuel reactivity controlled compression ignition (RCCI): a pathway to controlled high-efficiency clean combustion, Int. J. Engine Res. 12 (2011) 209–226.
- [5] S. J. Curran, R. M. Hanson, R. M. Wagner, Reactivity controlled compression ignition combustion on a multi-cylinder light-duty diesel engine, Int. J. Engine Res. 13 (2012) 216–225.
- [6] D. A. Splitter, R. D. Reitz, Fuel reactivity effects on the efficiency and operational window of dual-fuel compression ignition engines, Fuel 118 (2013) 163–175.
- [7] M. Yao, Z. Zheng, H. Liu, Progress and recent trends in homogeneous charge compression ignition (HCCI) engines, Prog. Energy Comb. Sci. 35 (2009) 398–437.
- [8] M. Noguchi, Y. Tanaka, T. Tanaka, Y. Takeuchi, A study on gasoline engine combustion by observation of intermediate reactive products during combustion, SAE Technical Paper 790840, 1979. doi:[10.4271/790840](https://doi.org/10.4271/790840).
- [9] F. Zhao, T. W. Asmus, D. N. Assanis, J. E. Dec, J. A. Eng, P. M. Najt, Homogeneous Charge Compression Ignition (HCCI) Engines: Key Research and Development Issues, PT-94, SAE International, Warrendale, PA, 2003.
- [10] M. Christensen, A. Hultqvist, B. Johansson, Demonstrating the multi fuel capability of a homogeneous charge compression ignition engine with variable compression ratio, SAE Technical Paper 1999-01-3679, 1999. doi:[10.4271/1999-01-3679](https://doi.org/10.4271/1999-01-3679).

- [11] T. Aroonsrisopon, V. Sohm, P. Werner, D. E. Foster, T. Morikawa, M. Iida, An investigation into the effect of fuel composition on HCCI combustion characteristics, SAE Technical Paper 2002-01-2830, 2002. doi:[10.4271/2002-01-2830](https://doi.org/10.4271/2002-01-2830).
- [12] P. E. Yelvington, M. B. I. Rallo, S. Liput, J. W. Tester, W. H. Green, J. Yang, Prediction of performance maps for homogeneous-charge compression-ignition engines, *Combust. Sci. Technol.* 176 (2004) 1243–1282.
- [13] M. J. Atkins, C. R. Koch, The effect of fuel octane and diluent on homogeneous charge compression ignition combustion, *Proc. IMechE. Part D: J. Automobile Engineering* 219 (2005) 665–675.
- [14] G. T. Kalghatgi, Auto-ignition quality of practical fuels and implications for fuel requirements of future SI and HCCI engines, SAE Technical Paper 2005-01-0239, 2005. doi:[10.4271/2005-01-0239](https://doi.org/10.4271/2005-01-0239).
- [15] G. Shibata, T. Urushihara, Auto-ignition characteristics of hydrocarbons and development of HCCI fuel index, SAE Technical Paper 2007-01-0220, 2007. doi:[10.4271/2007-01-0220](https://doi.org/10.4271/2007-01-0220).
- [16] T. Ogura, J. P. Angelos, W. H. Green, W. K. Cheng, T. Kenney, Y. Xu, Primary reference fuel behavior in a HCCI engine near the low-load limit, SAE Technical Paper 2008-01-1667, 2008. doi:[10.4271/2008-01-1667](https://doi.org/10.4271/2008-01-1667).
- [17] H. Liu, M. Yao, B. Zhang, Z. Zheng, Influence of fuel and operating conditions on combustion characteristics of a homogeneous charge compression ignition engine, *Energy Fuels* 23 (2009) 1422–1430.
- [18] L. Starck, B. Lecointe, L. Forti, N. Jeuland, Impact of fuel characteristics on HCCI combustion: Performances and emissions, *Fuel* 89 (2010) 3069–3077.
- [19] A. M. Aldawood, S. Mosbach, M. Kraft, A. A. Amer, Dual-fuel effects on HCCI operating range: Experiments with primary reference fuels, SAE Technical Paper 2013-01-1673, 2013. doi:[10.4271/2013-01-1673](https://doi.org/10.4271/2013-01-1673).
- [20] X. Han, M. Zheng, J. Wang, Fuel suitability for low temperature combustion in compression ignition engines, *Fuel* 109 (2013) 336–349.
- [21] J. S. Lacey, Z. S. Filipi, S. R. Sathasivam, W. J. Cannella, P. A. Fuentes-Afflick, HCCI operability limits: The impact of refinery stream gasoline property variation, *J. Eng. Gas. Turb. Power* 135 (2013) 081505.
- [22] V. H. Rapp, W. J. Cannella, J.-Y. Chen, R. W. Dibble, Predicting fuel performance for future HCCI engines, *Combust. Sci. Technol.* 185 (2013) 735–748.
- [23] I. Truedsson, W. Cannella, B. Johansson, M. Tuner, Development of new test method for evaluating HCCI fuel performance, SAE Technical Paper 2014-01-2667, 2014. doi:[10.4271/2014-01-2667](https://doi.org/10.4271/2014-01-2667).
- [24] C. K. W. Ng, M. J. Thomson, A computational study of the effect of fuel reforming, EGR and initial temperature on lean ethanol HCCI combustion, SAE Technical Paper 2004-01-0556, 2004. doi:[10.4271/2004-01-0556](https://doi.org/10.4271/2004-01-0556).
- [25] M. Sjöberg, J. E. Dec, Ethanol autoignition characteristics and HCCI performance for wide ranges of engine speed, load and boost, *SAE Int. J. Engines* 3 (2010) 84–106.
- [26] R. K. Maurya, A. K. Agarwal, Experimental study of combustion and emission characteristics of ethanol fuelled port injected homogeneous charge compression ignition (HCCI) combustion engine, *Applied Energy* 88 (2011) 1169–1180.
- [27] J. H. Mack, S. M. Aceves, R. W. Dibble, Demonstrating direct use of wet ethanol in a homogeneous charge compression ignition (HCCI) engine, *Energy* 34 (2009) 782–787.
- [28] J. Martinez-Frias, S. M. Aceves, D. L. Flowers, Improving ethanol life cycle energy efficiency by direct utilization of wet ethanol in HCCI engines, *J. Energy Resour. Technol.* 129 (2007) 332–337.

- [29] A. Megaritis, D. Yap, M. L. Wyszynski, Effect of water blending on bioethanol HCCI combustion with forced induction and residual gas trapping, *Energy* 32 (2007) 2396–2400.
- [30] K. Hashimoto, Effect of ethanol on the HCCI combustion, SAE Technical Paper 2007-01-2038, 2007. doi:[10.4271/2007-01-2038](https://doi.org/10.4271/2007-01-2038).
- [31] J. H. Mack, D. L. Flowers, B. A. Buchholz, R. W. Dibble, Investigation of HCCI combustion of diethyl ether and ethanol mixtures using carbon 14 tracing and numerical simulations, *Proc. Combust. Inst.* 30 (2005) 2693–2700.
- [32] S. Mosbach, M. Kraft, A. Bhave, F. Mauss, J. H. Mack, R. W. Dibble, Simulating a homogeneous charge compression ignition engine fuelled with a DEE/EtOH blend, SAE Technical Paper 2006-01-1362, 2006. doi:[10.4271/2006-01-1362](https://doi.org/10.4271/2006-01-1362).
- [33] H. Ogawa, N. Miyamoto, N. Kaneko, H. Ando, Combustion control and operating range expansion with direct injection of reaction suppressors in a premixed DME HCCI engine, SAE Technical Paper 2003-01-0746, 2003. doi:[10.4271/2003-01-0746](https://doi.org/10.4271/2003-01-0746).
- [34] H. Yamada, M. Yoshii, A. Tezaki, Chemical mechanistic analysis of additive effects in homogeneous charge compression ignition of dimethyl ether, *Proc. Combust. Inst.* 30 (2005) 2773–2780.
- [35] M. Yao, Z. Chen, Z. Zheng, B. Zhang, Y. Xing, Study on the controlling strategies of homogeneous charge compression ignition combustion with fuel of dimethyl ether and methanol, *Fuel* 85 (2006) 2046–2056.
- [36] M. Yao, C. Huang, Z. Zheng, Multidimensional numerical simulation on dimethyl ether/methanol dual-fuel homogeneous charge compression ignition (HCCI) engine combustion and emission processes, *Energy Fuels* 21 (2007) 812–821.
- [37] J. H. Mack, R. W. Dibble, B. A. Buchholz, D. L. Flowers, The effect of the di-tertiary butyl peroxide (DTBP) additive on HCCI combustion of fuel blends of ethanol and diethyl ether, SAE Technical Paper 2005-01-2135, 2005. doi:[10.4271/2005-01-2135](https://doi.org/10.4271/2005-01-2135).
- [38] M. Christensen, B. Johansson, Homogeneous charge compression ignition with water injection, SAE Technical Paper 1999-01-0182, 1999. doi:[10.4271/1999-01-0182](https://doi.org/10.4271/1999-01-0182).
- [39] Y. Iwashiro, T. Tsurushima, Y. Nishijima, Y. Asaumi, Y. Aoyagi, Fuel consumption improvement and operation range expansion in HCCI by direct water injection, SAE Technical Paper 2002-01-0105, 2002. doi:[10.4271/2002-01-0105](https://doi.org/10.4271/2002-01-0105).
- [40] T. Steinhilber, T. Sattelmayer, The effect of water addition on HCCI diesel combustion, SAE Technical Paper 2006-01-3321, 2006. doi:[10.4271/2006-01-3321](https://doi.org/10.4271/2006-01-3321).
- [41] A. Viggiano, V. Magi, A comprehensive investigation on the emissions of ethanol HCCI engines, *Applied Energy* 93 (2012) 277–287.
- [42] K. E. Niemeyer, S. R. Daly, W. J. Cannella, C. L. Hagen, A novel fuel performance index for low-temperature combustion engines based on operating envelopes in light-duty driving cycle simulations, *J. Eng. Gas. Turb. Power* 137 (2015) 101601.
- [43] H. Zhao, J. Li, T. Ma, N. Ladommatos, Performance and analysis of a 4-stroke multi-cylinder gasoline engine with CAI combustion, SAE Technical Paper 2002-01-0420, 2002. doi:[10.4271/2002-01-0420](https://doi.org/10.4271/2002-01-0420).
- [44] S. J. Curran, K. Cho, T. E. Briggs, R. M. Wagner, Drive cycle efficiency and emissions estimates for reactivity controlled compression ignition in a multi-cylinder light-duty diesel engine, in: *ASME 2011 Internal Combustion Engine Division Fall Technical Conference (ICEF2011)*, ICEF2011-60227, Morgantown, WV, 2011, pp. 557–564. doi:[10.1115/ICEF2011-60227](https://doi.org/10.1115/ICEF2011-60227).

- [45] T. Kenney, T. P. Gardner, S. S. Low, J. C. Eckstrom, L. R. Wolf, S. J. Korn, P. G. Szymkowicz, Overall results: Phase I ad hoc diesel fuel test program, SAE Technical Paper 2001-01-0151, 2001. doi:[10.4271/2001-01-0151](https://doi.org/10.4271/2001-01-0151).
- [46] P. G. Szymkowicz, D. T. French, C. C. Crellin, Effects of advanced fuels on the particulate and NO_x emissions from an optimized light-duty CIDI engine, SAE Technical Paper 2001-01-0148, 2001. doi:[10.4271/2001-01-0148](https://doi.org/10.4271/2001-01-0148).
- [47] E. Ortiz-Soto, D. N. Assanis, A. Babajimopoulos, A comprehensive engine to drive-cycle modelling framework for the fuel economy assessment of advanced engine and combustion technologies, *Int. J. Engine Res.* 13 (2012) 287–304.
- [48] Z. Gao, C. S. Daw, R. M. Wagner, K. D. Edwards, D. E. Smith, Simulating the impact of premixed charge compression ignition on light-duty diesel fuel economy and emissions of particulates and NO_x, *Proc. IMechE. Part D: J. Automobile Engineering* 227 (2013) 31–51.
- [49] K. Ahn, J. Whitefoot, A. Babajimopoulos, E. Ortiz-Soto, P. Y. Papalambros, Homogeneous charge compression ignition technology implemented in a hybrid electric vehicle: System optimal design and benefit analysis for a power-split architecture, *Proc. IMechE. Part D: J. Automobile Engineering* 227 (2012) 87–98.
- [50] I. Truedsson, M. Tuner, B. Johansson, W. Cannella, Pressure sensitivity of HCCI auto-ignition temperature for primary reference fuels, *SAE Int. J. Engines* 5 (2012) 1089–1108.
- [51] I. Truedsson, M. Tuner, B. Johansson, W. Cannella, Emission formation study of HCCI combustion with gasoline surrogate fuels, SAE Technical Paper 2013-01-2626, 2013. doi:[10.4271/2013-01-2626](https://doi.org/10.4271/2013-01-2626).
- [52] I. Truedsson, M. Tuner, B. Johansson, W. Cannella, Pressure sensitivity of HCCI auto-ignition temperature for oxygenated reference fuels, *J. Eng. Gas. Turb. Power* 135 (2013) 072801.
- [53] EPA Office of Transportation and Air Quality, Dynamometer drive schedules, <http://www.epa.gov/nvfel/testing/dynamometer.htm>, 2013.
- [54] K. B. Wipke, M. R. Cuddy, S. D. Burch, ADVISOR 2.1: A user-friendly advanced powertrain simulation using a combined backward/forward approach, *IEEE Trans. Vehicular Technol.* 48 (1999) 1751–1761.
- [55] T. Markel, A. Brooker, T. Hendricks, V. Johnson, ADVISOR: a systems analysis tool for advanced vehicle modeling, *J. Power Sources* 110 (2002) 255–266.
- [56] D. W. Gao, C. Mi, A. Emadi, Modeling and simulation of electric and hybrid vehicles, *Proc. IEEE* 95 (2007) 729–745.
- [57] D. Reilly, R. Andersen, R. Casparian, P. Dugdale, Saturn DOHC and SOHC four cylinder engines, SAE Technical Paper 910676, 1991. doi:[10.4271/910676](https://doi.org/10.4271/910676).
- [58] J. B. Heywood, *Internal Combustion Engine Fundamentals*, McGraw-Hill, New York, 1988.
- [59] H. W. Barnes-Moss, A designer’s viewpoint, in: *Passenger Car Engines*, Conference Proceedings, Institution of Mechanical Engineers, London, England, UK, 1975, pp. 133–147.
- [60] K. J. Patton, R. G. Nitschke, J. B. Heywood, Development and evaluation of a friction model for spark-ignition engines, SAE Technical Paper 890836, 1989. doi:[10.4271/890836](https://doi.org/10.4271/890836).
- [61] D. A. Kouremenos, C. D. Rakopoulos, D. T. Hountalas, T. K. Zannis, Development of a detailed friction model to predict mechanical losses at elevated maximum combustion pressures, SAE Technical Paper 2001-01-0333, 2001. doi:[10.4271/2001-01-0333](https://doi.org/10.4271/2001-01-0333).
- [62] D. Sandoval, J. B. Heywood, An improved friction model for spark-ignition engines, SAE Technical Paper 2003-01-0725, 2003. doi:[10.4271/2003-01-0725](https://doi.org/10.4271/2003-01-0725).

- [63] R. A. Mufti, M. Priest, R. J. Chittenden, Analysis of piston assembly friction using the indicated mean effective pressure experimental method to validate mathematical models, *Proc. IMechE. Part D: J. Automobile Engineering* 222 (2008) 1441–1457.
- [64] Reaction Design, CHEMKIN 10131, San Diego, 2013.
- [65] N. Milovanovic, R. Chen, J. Turner, Influence of the variable valve timing strategy on the control of a homogeneous charge compression (HCCI) engine, SAE Technical Paper 2004-01-1899, 2004. doi:[10.4271/2004-01-1899](https://doi.org/10.4271/2004-01-1899).
- [66] J. R. Zuehl, J. Ghandhi, C. L. Hagen, W. J. Cannella, Fuel effects on HCCI combustion using negative valve overlap, SAE Technical Paper 2010-01-0161, 2010. doi:[10.4271/2010-01-0161](https://doi.org/10.4271/2010-01-0161).
- [67] D. L. Flowers, S. M. Aceves, R. Smith, J. Torres, J. Girard, R. W. Dibble, HCCI in a CFR engine: Experiments and detailed kinetic modeling, SAE Technical Paper 2000-01-0328, 1999. doi:[10.4271/2000-01-0328](https://doi.org/10.4271/2000-01-0328).
- [68] H. Zhao (Ed.), HCCI and CAI engines for the automotive industry, Woodhead Publishing, Cambridge England, 2007.
- [69] S. Saxena, I. D. Bedoya, Fundamental phenomena affecting low temperature combustion and HCCI engines, high load limits and strategies for extending these limits, *Prog. Energy Comb. Sci.* 39 (2013) 457–488.
- [70] A. Aldawood, S. Mosbach, M. Kraft, HCCI combustion control using dual-fuel approach: Experimental and modeling investigations, SAE Technical Paper 2012-01-1117, 2012. doi:[10.4271/2012-01-1117](https://doi.org/10.4271/2012-01-1117).
- [71] J. A. Eng, Characterization of pressure waves in HCCI combustion, SAE Technical Paper 2002-01-2859, 2002. doi:[10.4271/2002-01-2859](https://doi.org/10.4271/2002-01-2859).
- [72] J. E. Dec, Y. Yang, Boosted HCCI for high power without engine knock and with ultra-low NOx emissions - using conventional gasoline, *SAE Int. J. Engines* 3 (2010) 750–767.
- [73] A. Oakley, H. Zhao, N. Ladommatos, T. Ma, Experimental studies on controlled auto-ignition (CAI) combustion of gasoline in a 4-stroke engine, SAE Technical Paper 2001-01-1030, 2001. doi:[10.4271/2001-01-1030](https://doi.org/10.4271/2001-01-1030).
- [74] P. Yelvington, W. Green, Prediction of the knock limit and viable operating range for a homogeneous-charge compression-ignition (HCCI) engine, SAE Technical Paper 2003-01-1092, 2003. doi:[10.4271/2003-01-1092](https://doi.org/10.4271/2003-01-1092).
- [75] I. Truedsson, The HCCI Fuel Number: Measuring and Describing Auto-ignition for HCCI Combustion Engines, Ph.D. thesis, Lund University, 2014.
- [76] R. H. Butt, Y. Chen, J. H. Mack, S. Saxena, R. W. Dibble, J.-Y. Chen, Improving ion current of sparkplug ion sensors in HCCI combustion using sodium, potassium, and cesium acetates: Experimental and numerical modeling, *Proc. Combust. Inst.* 35 (2015) 3107–3115.
- [77] E. Jones, T. Oliphant, P. Peterson, et al., SciPy: Open source scientific tools for Python, <http://www.scipy.org/>, 2001–. [Online; accessed 2014-09-03].
- [78] C. B. Barber, D. P. Dobkin, H. Huhdanpaa, The quickhull algorithm for convex hulls, *ACM Trans. Math. Software* 22 (1996) 469–483.
- [79] Z. Gao, J. C. Conklin, C. S. Daw, V. K. Chakravarthy, A proposed methodology for estimating transient engine-out temperature and emissions from steady-state maps, *Int. J. Engine Res.* 11 (2010) 137–151.
- [80] S. Nüesch, E. Hellström, L. Jiang, A. Stefanopoulou, Influence of transitions between SI and HCCI combustion on driving cycle fuel consumption, in: *European Control Conference*, Zurich, Switzerland, 2013, pp. 1976–1981.

- [81] S. M. Aceves, D. L. Flowers, C. K. Westbrook, J. R. Smith, W. J. Pitz, R. W. Dibble, M. Christensen, A multi-zone model for prediction of HCCI combustion and emissions, SAE Technical Paper 2000-01-0327, 2000. doi:[10.4271/2000-01-0327](https://doi.org/10.4271/2000-01-0327).
- [82] S. B. Fiveland, D. N. Assanis, Development of a two-zone HCCI combustion model accounting for boundary layer effects, SAE Technical Paper 2001-01-1028, 2001. doi:[10.4271/2001-01-1028](https://doi.org/10.4271/2001-01-1028).
- [83] G. Chin, J.-Y. Chen, Modeling of emissions from HCCI engines using a consistent 3-zone model with applications to validation of reduced chemistry, *Proc. Combust. Inst.* 33 (2011) 3073–3079.
- [84] J. Kodavasal, M. J. McNenly, A. Babajimopoulos, S. M. Aceves, D. N. Assanis, M. A. Havstad, D. L. Flowers, An accelerated multi-zone model for engine cycle simulation of homogeneous charge compression ignition combustion, *Int. J. Engine Res.* 14 (2013) 416–433.
- [85] M. Chaos, A. Kazakov, Z. Zhao, F. L. Dryer, A high-temperature chemical kinetic model for primary reference fuels, *Int. J. Chem. Kinet.* 39 (2007) 399–414.
- [86] M. Chaos, Z. Zhao, A. Kazakov, P. Gokulakrishnan, M. Angioletti, F. L. Dryer, A PRF+toluene surrogate fuel model for simulating gasoline kinetics, in: Fifth Joint Meeting of the US Sections of the Combustion Institute, Paper E26, 2007.
- [87] J. Li, A. Kazakov, M. Chaos, F. L. Dryer, Chemical kinetics of ethanol oxidation, in: Fifth Joint Meeting of the US Sections of the Combustion Institute, Paper C28, San Diego, CA, 2007.
- [88] F. M. Haas, M. Chaos, F. L. Dryer, Low and intermediate temperature oxidation of ethanol and ethanol-PRF blends: An experimental and modeling study, *Combust. Flame* 156 (2009) 2346–2350.
- [89] K. E. Niemeyer, vol-to-mole, figshare, 2014. doi:[10.6084/m9.figshare.1221842](https://doi.org/10.6084/m9.figshare.1221842).
- [90] J. A. Eng, W. R. Leppard, P. M. Najt, T.-W. Kuo, Fuel adaptation in a homogeneous charge compression ignition engine, US Patent 2007/0119417A1, 2007.
- [91] S. Saxena, J.-Y. Chen, R. Dibble, Maximizing power output in an automotive scale multi-cylinder homogeneous charge compression ignition (HCCI) engine, SAE Technical Paper 2011-01-0907, 2011. doi:[10.4271/2011-01-0907](https://doi.org/10.4271/2011-01-0907).
- [92] S. Saxena, N. Shah, I. Bedoya, A. Phadke, Understanding optimal engine operating strategies for gasoline-fueled HCCI engines using crank-angle resolved exergy analysis, *Applied Energy* 114 (2014) 155–163.
- [93] N. Morgan, A. J. Smallbone, A. Bhave, M. Kraft, R. Cracknell, G. T. Kalghatgi, Mapping surrogate gasoline compositions into RON/MON space, *Combust. Flame* 157 (2010) 1122–1131.
- [94] B. M. Gauthier, D. F. Davidson, R. K. Hanson, Shock tube determination of ignition delay times in full-blend and surrogate fuel mixtures, *Combust. Flame* 139 (2004) 300–311.